

See discussions, stats, and author profiles for this publication at: <https://www.researchgate.net/publication/223729533>

# Temporal and spatial variability of Chl-a and SST on the South Atlantic Bight: Revisiting with cloud-free reconstructions of MODIS satellite imagery

ARTICLE *in* CONTINENTAL SHELF RESEARCH · OCTOBER 2010

Impact Factor: 1.89 · DOI: 10.1016/j.csr.2010.08.016

---

CITATIONS

11

READS

42

---

## 2 AUTHORS:



Travis N Miles

Rutgers, The State University of New Jersey

15 PUBLICATIONS 40 CITATIONS

[SEE PROFILE](#)



Ruoying He

North Carolina State University

100 PUBLICATIONS 1,438 CITATIONS

[SEE PROFILE](#)



## Research papers

Temporal and spatial variability of Chl-*a* and SST on the South Atlantic Bight: Revisiting with cloud-free reconstructions of MODIS satellite imagery

Travis N. Miles, Ruoying He\*

*Department of Marine, Earth & Atmospheric Sciences, North Carolina State University, Raleigh, NC, USA*

## ARTICLE INFO

## Article history:

Received 19 August 2009

Received in revised form

27 July 2010

Accepted 18 August 2010

Available online 16 September 2010

## Keywords:

Coastal oceanography

Satellite observations

SST and CHL-*a* variability

South Atlantic Bight

## ABSTRACT

Daily, cloud-free data interpolating empirical orthogonal function (DINEOF) reconstructions of sea-surface temperature (SST) and chlorophyll (Chl-*a*) satellite imagery are compiled into monthly mean images for a six-year period (2003–2008) and used to identify their spatial and temporal variability on the South Atlantic Bight. Monthly-mean SST has the highest variability on the inner-shelf, decreasing seaward approaching the more stable temperatures of the Gulf Stream (GS). Monthly-mean Chl-*a* concentrations are similarly highest on the inner shelf throughout the year and decrease cross-shelf toward the nutrient depleted open ocean. Empirical orthogonal function (EOF) analyses on SST and Chl-*a* show a clear seasonal cycle in their 1st mode of variability, with SST lagging behind Chl-*a* by approximately one month. The 1st EOF modes account for 95.8% and 46.4% variance of SST and Chl-*a*, respectively. Chl-*a* EOF mode 1 in particular shows a highly regionalized spatial pattern with values on the central SAB clearly out of phase with the southern and northern SAB. This regional difference is likely a result of shelf geometry and stratification, which modulate GS influence on the shelf. SST EOF mode 2 exhibits a seasonal cycle as well, which previous studies have shown to be a function of local wind. Chl-*a* EOF mode 2 is well correlated with the cumulative river transport onto the SAB, but accounts for a relatively small 10.8% of Chl-*a* variability.

© 2010 Elsevier Ltd. All rights reserved.

## 1. Introduction

The South Atlantic Bight (SAB) stretches from Cape Canaveral, Florida, to Cape Hatteras, North Carolina, accounting for approximately 700 km of coastline between 28°N and 35°N (Fig. 1). Shelf widths are at a maximum in the central SAB off the coast of Georgia, reaching approximately 120 km offshore. Off Cape Canaveral and Cape Hatteras, shelf-widths are at a minimum, being only about 10–30 km. A topographic ridge known as the Charleston Bump is present at 32°N off the coast of Charleston, South Carolina. In terms of ocean circulation dynamics, the SAB can be subdivided into the inner shelf (~0–20 m), middle shelf (~20–40 m), outer shelf (~40–70 m) and shelf slope (~70–200 m) (Atkinson and Menzel, 1985). The inner shelf connects to estuaries, rivers and salt marshes and is influenced most strongly by tidal, river and local wind forcing. In contrast, the outer shelf and shelf slope are predominately driven by the Gulf Stream (Lee et al., 1991). The middle shelf receives combined influence from river discharge, the Gulf Stream, wind, heat flux and tidal forcing (e.g., Arexabaleta et al., 2006).

Inner shelf sea surface temperature (SST) follows air temperature, while both the GS and surface winds modulate water temperature on the middle and outer shelves. Previous studies indicate minimum surface temperatures (~10 °C) on the inner shelf occur in late winter and early spring (Oey et al., 1987). The middle shelf of the SAB reaches maximum temperatures of ~28 °C in summer, when the thermocline is shallow and the shelf is highly stratified. The presence of persistently warm GS water leads to strong cross-shelf thermal gradients in winter and weaker gradients in summer along the entire shelf (Atkinson, 1985; Signorini and McClain, 2006; Signorini and McClain, 2007).

Atkinson (1985), Yoder et al. (1985) and Bishop et al. (1980) show that nutrients enter the SAB from a variety of sources. Because of shallow depths and energetic mixing on the SAB, unlike in other coastal regimes such as the Middle Atlantic Bight, phytoplankton use nutrients quickly before a near-bottom nutrient pool can develop. The primary nutrient sources of the SAB are Gulf Stream (GS) intrusions. Upwelling-favorable winds during spring and summer can further enhance such intrusions, bringing more nutrient-rich North Atlantic bottom water onto the outer shelf (Atkinson, 1977, 1984, 1985; Blanton, 1981; Yoder et al., 1985). The density front created by freshwater runoff serves as a buffer that largely isolates the inner shelf from upwelled nutrients (Yoder et al., 1985). Instead, nutrients enter the inner shelf primarily through rivers and estuaries along the central to

\* Corresponding author. Tel.: +1 919 513 0249.

E-mail address: rhe@ncsu.edu (R. He).

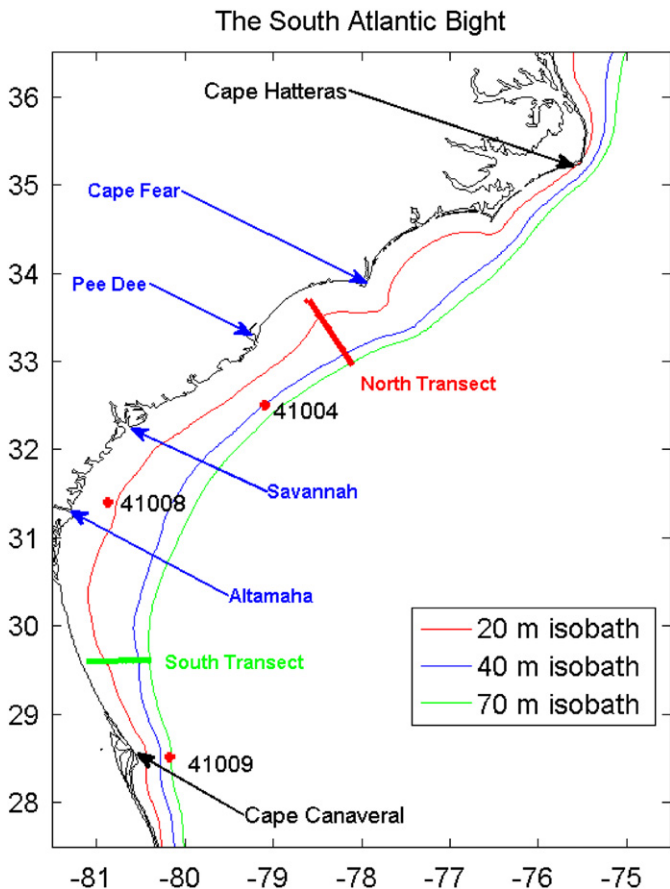


**Fig. 1.** The South Atlantic Bight from Cape Canaveral to Cape Hatteras. Isobath lines mark the inner shelf (0–20 m), middle shelf (20–40 m), outer shelf (40–70 m). Blue arrows indicate major river locations. Red dots indicate buoy locations, while the thick red line and thick green line represent North and South transects discussed in Fig. 7. (For interpretation of the references to color in this figure legend, the reader is referred to the web version of this article.)

northern SAB. Maximum river runoff occurs in March facilitating a spring phytoplankton bloom (Atkinson and Menzel, 1985). The narrow shelf and less freshwater discharge south of Jacksonville, Florida, lead to a limited density front and enhanced interaction between the shelf and the GS. As a result, GS influences are present in this region during all seasons through frontal eddies and meanders (Yoder, 1985).

Consistent with surface nutrient distribution, surface chlorophyll concentrations are highest in coastal waters with an annual mean of over  $1.0 \text{ mg/m}^3$  on the inner shelf. Chlorophyll concentration decreases to approximately  $0.3 \text{ mg/m}^3$  at the shelf-break toward the nutrient depleted GS surface waters. Shelf-break upwelling can sometimes inject nutrients into the upper water column and lead to a narrow band of elevated chlorophyll concentration on the outer shelf during fall and winter months (Barnard et al., 1997; Ryan and Yoder, 1996). North of Jacksonville, Florida, river transport of nutrients can significantly affect chlorophyll concentration. Elevated chlorophyll concentration and the large cross-shelf extent of blooms correspond with times of elevated runoff of major rivers in the central SAB, such as the Pee Dee River and the Cape Fear River.

The temporal and spatial variability of regional Chl-a and SST have been investigated in the past. Barnard et al. (1997) used coastal zone color scanner (CZCS) and advanced very high resolution radiometer (AVHRR) sensors to study the variability of ocean-color and surface temperature in the northern SAB.

They identified a surface seasonal signal of Chl-a in the northern SAB that leads SST seasonal variability by approximately one month. This was the first study to use long-term satellite data sets to examine the seasonal characteristics of SST and Chl-a in the SAB. The Barnard et al., 1997 study however was limited by a small set of available satellite images. Over their five-year study period (1981–1986), only 372 CZCS chlorophyll and 866 AVHRR SST images were retained to represent SST and Chl-a seasonal signals. In recent years, the National Aeronautics and Space Administration (NASA) has developed more advanced sensors to resolve the ocean surface signal. Among them, the moderate resolution imaging spectroradiometer (MODIS) sensor was launched in 2002 aboard the Earth Observing Satellite, Aqua. Since its inception MODIS has been continuously retrieving high resolution, daily images of SST and Chl-a. One unique feature of MODIS is that SST and Chl-a are measured concurrently, providing ideal data sets to examine the spatial and temporal co-variability between temperature and ocean-color fields. Cloud-cover is still a limiting factor for data collection, but new data analysis techniques described in Alvera-Azcarate et al. (2007) and Miles et al. (2009) provide an effective cloud removing procedure. The resulting large amount of daily, cloud-free MODIS SST and Chl-a images make an excellent product for an updated study of surface ocean variability on the SAB. As previous studies (e.g., Barnard et al., 1997) utilize limited remote sensing data sets, it also seems prudent to revisit their findings.

We focus on the time period from 2003 to 2008 for the SAB. Different from Barnard et al.'s (1997) study, which considered a sub-regional domain constrained to the northern SAB from approximately  $32.5^\circ\text{N}$  to  $36.5^\circ\text{N}$ , our study region includes the entire SAB from Cape Canaveral, Florida to Cape Hatteras, North Carolina to examine the latitudinal regional differences in ocean surface signals.

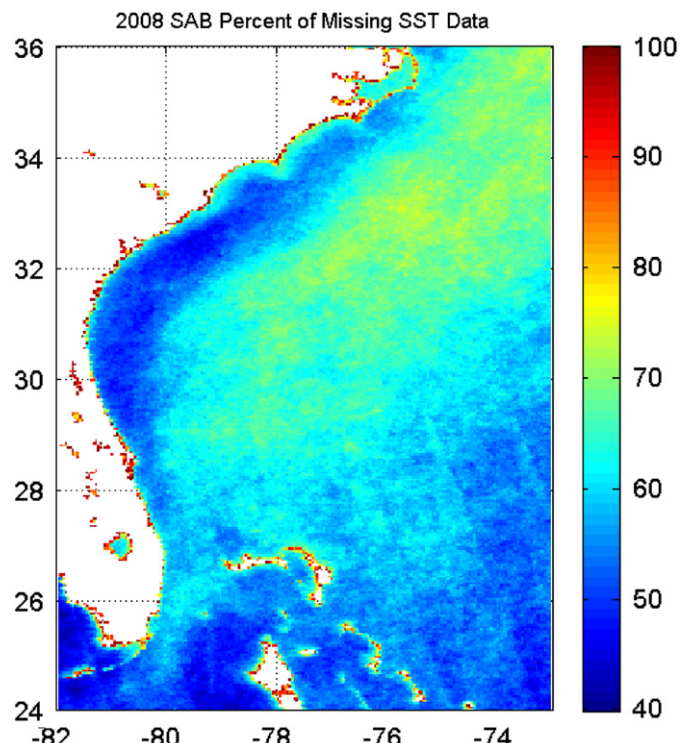


**Fig. 2.** The percentage of cloud-covered SST data missing in the 2008 MODIS data set.

## 2. Data and methods

MODIS Aqua 4 micron daytime SST and Chl-a Level 3 products are gridded to a  $384 \times 215$  pixel grid, identical to the grid used in Miles et al. (2009). We collected these satellite images, which have

a 4 km resolution, from NASA Goddard Space Flight Center. The data set includes the time period from January 1, 2003, to December 31, 2008. MODIS is only capable of viewing in the visible and infrared wave bands; thus almost all images have cloud cover to various extents. Prior to cloud-free reconstruction,

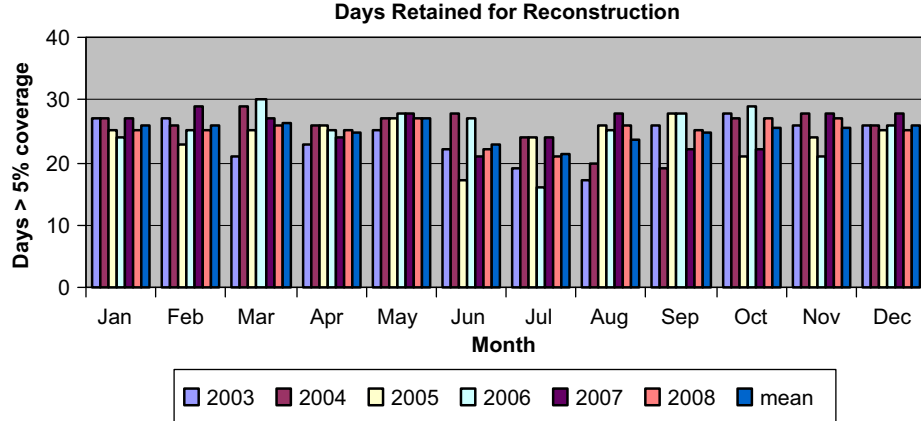


Fig. 3. Total days of images retained for DINEOF reconstruction. Retained images have over 5% data coverage.

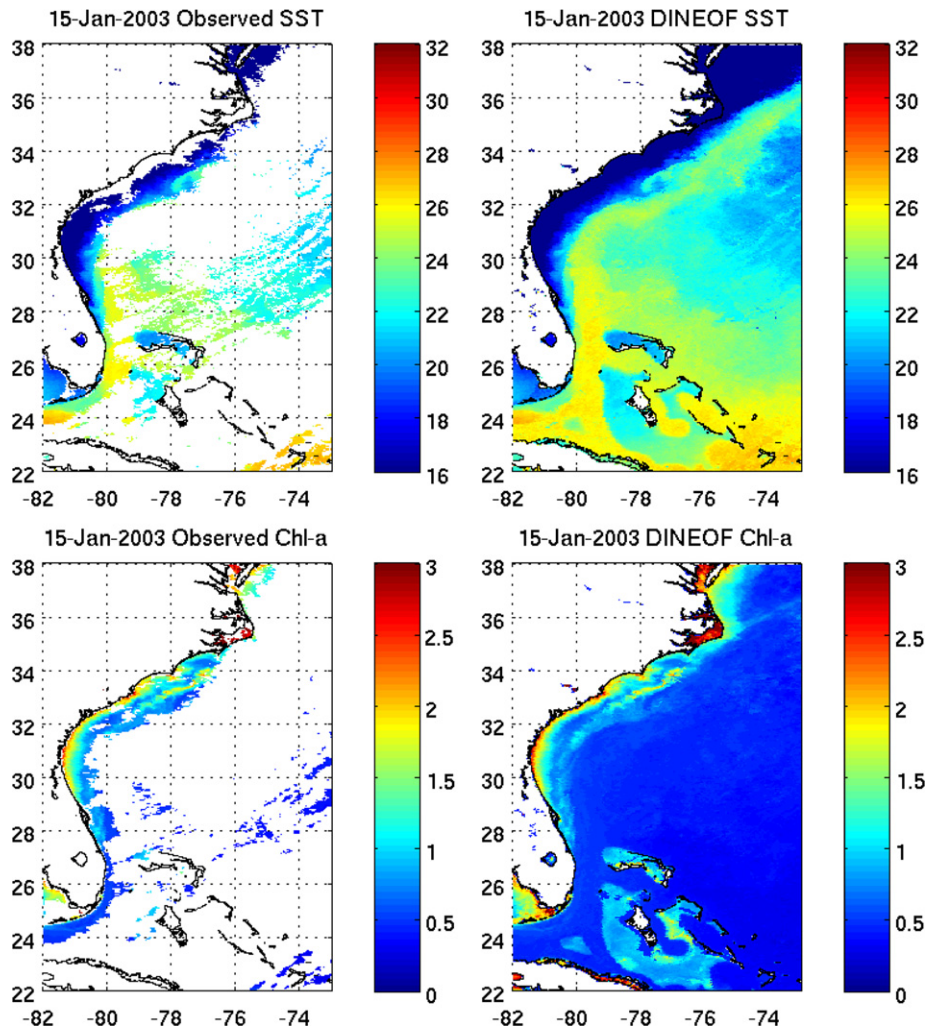
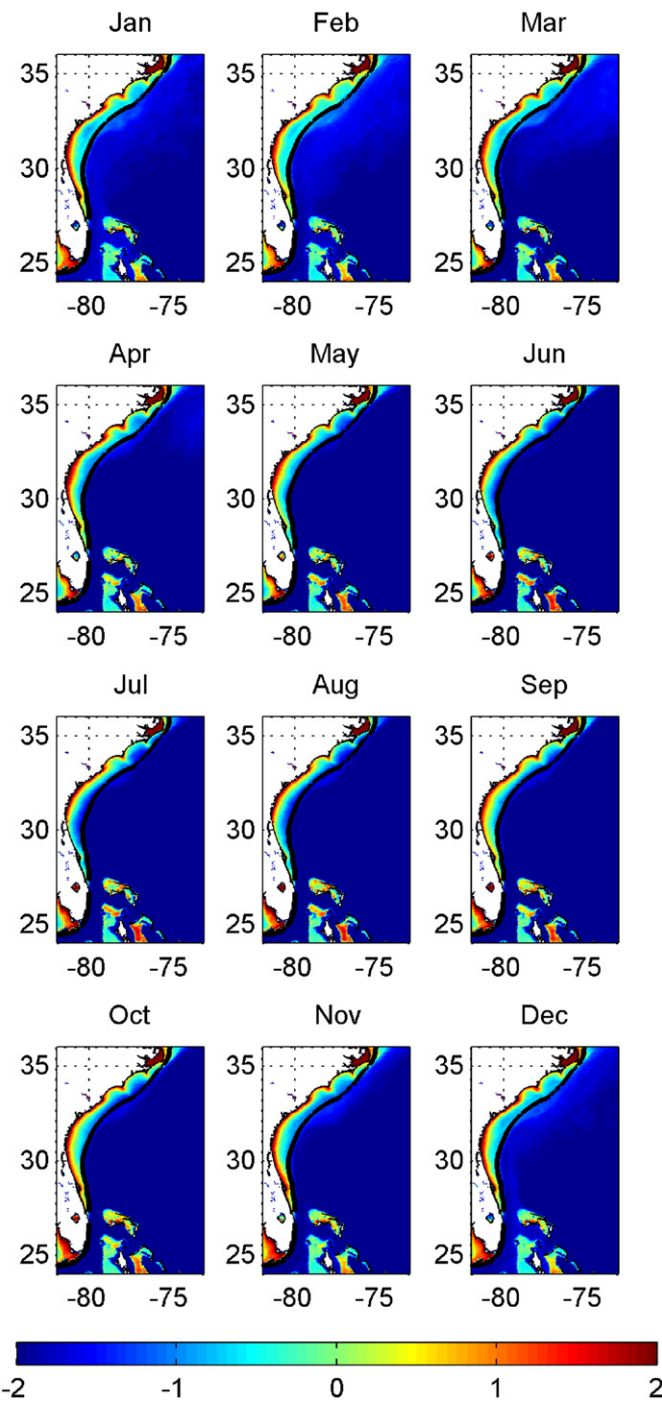


Fig. 4. A snapshot of raw SST ( $^{\circ}\text{C}$ ) and Chl-a ( $\text{mg}/\text{m}^3$ ) (upper left and lower left, respectively) with DINEOF reconstructed SST and Chl-a (upper right and lower right, respectively). There is a notable shelf-break Chl-a bloom, which typically persists from November to March in daily imagery.

satellite data on the SAB are missing 60% of the time in coastal regions and up to 80% of the time toward the deep-ocean, due to cloud-cover (Fig. 2). The high missing data rate offshore is presumed to be due to stronger convection over the warm GS waters. We removed images with less than 5% data coverage from the Chl-*a* and SST data sets prior to processing, as images with more than 95% cloud-cover harm reconstruction quality (Alvera-Azcarate et al., 2007). As a result, we retained 1801 of the initial 2192 daily images. The mean number of images retained in each month is 25 (Fig. 3), with a minimum in satellite coverage in July (of ~20 images) and maximum coverage in May (of ~28 images).



**Fig. 5.** Natural log of monthly mean Chl-*a* ( $\text{mg}/\text{m}^3$ ) derived from 2003 to 2008 MODIS daily DINEOF reconstructed imagery. The black contour indicates the 70 m isobath.

We performed a cloud-free data reconstruction using the DINEOF method. This method identifies dominant spatial and temporal patterns in SST and Chl-*a* data sets and fills in missing data accordingly. Unlike other reconstruction techniques (e.g., optimal interpolation (OI) method used by He et al., 2003), this method requires no *a priori* information on decorrelation scales and can use multiple data types with inherent correlations to increase spatial and temporal data coverage. Miles et al. (2009) showed that the DINEOF method provides results statistically similar to OI reconstruction methods but 30 times faster. We refer interested readers to Alvera-Azcarate et al. (2007) for details of

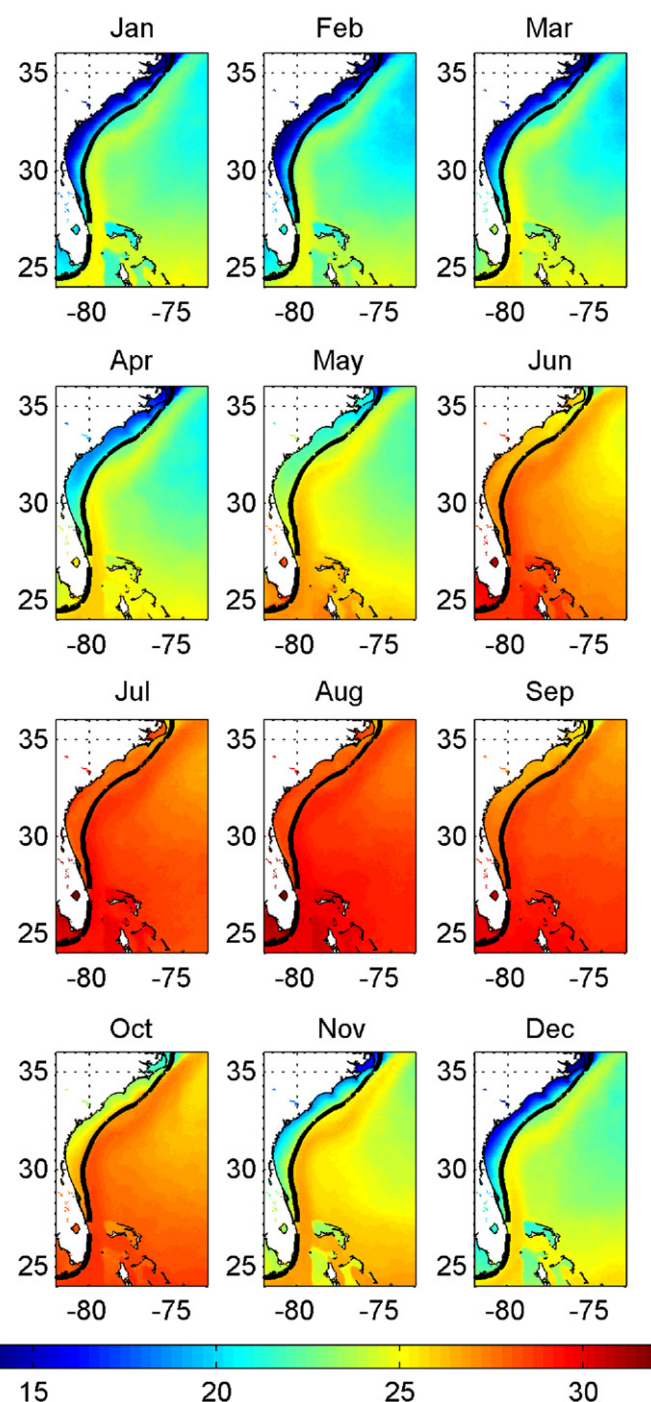


**Fig. 6.** Monthly mean SST ( $^{\circ}\text{C}$ ) derived from 2003 to 2008 MODIS daily DINEOF reconstructed imagery. The black contour indicates the 70 m isobath.

the DINEOF method. Appendix A provides a brief methods description. In this study, we applied the exact multivariate DINEOF approach used in Miles et al. (2009). The resulting six years (2003–2008) of daily reconstructions are available online at: [omglnx2.meas.ncsu.edu/travis/DINEOF/](http://omglnx2.meas.ncsu.edu/travis/DINEOF/). We note that DINEOF reconstruction requires a normally distributed dataset, therefore to accurately reconstruct Chl-a fields, we calculated the natural logarithm of concentrations first. Miles et al. 2009 provides validation statistics comparing the DINEOF SST reconstruction against buoy measured SST in the SAB. In that study it was found that their correlation coefficients are above 0.93 with the seasonal signal retained and above 0.59 with it removed, demonstrating the utility of this reconstruction method. Following the six years of daily, cloud-free reconstruction, we then computed monthly means of SST and Chl-a fields for the entire SAB.

Other data sets used in this study include United States Geological Survey (USGS) river gauge flow observations. We obtain daily river discharge (<http://waterdata.usgs.gov>) from 2003 to 2008 for four major rivers in the SAB: the Cape Fear, Pee Dee, Altamaha and Savannah (Fig. 1), which we then compiled into their corresponding monthly means. We also calculated the cumulative transport from these rivers to estimate the total freshwater transport onto the SAB.

In order to account for the influence of wind forcing on the SAB ocean surface conditions, we also utilized monthly mean North Atlantic Regional Reanalysis (NARR) wind fields over the SAB from 2003 to 2008. 6-hourly NARR winds are provided by the National Centers for Environmental Protection (NCEP: <http://www.cdc.noaa.gov>) at 32 km spatial resolution.

### 3. Results

A daily snapshot of raw and DINEOF reconstructed Chl-a and SST is given in Fig. 4 (similar results for the entire dataset can be found on our website mentioned in Section 2). This image clearly shows the utility of the DINEOF method in reconstructing daily high-resolution imagery from data sets with large amounts of cloud-cover. For example, in the Chl-a reconstruction, we observed a persistent thin band of elevated chlorophyll during winter and early spring at the shelf-break. Barnard et al. (1997) and Ryan and Yoder (1996) previously related this narrow band to synoptic upwelling from the GS interaction with the shelf-break.

Figs. 5 and 6 show the six-year (2003–2008) means for each month for Chl-a and SST, respectively. While such long-term averaging removed synoptic features, the resulting mean fields represent the climatological states of the SAB Surface Ocean. All Chl-a monthly means follow a similar pattern, with highest chlorophyll concentrations on the shallow shelf decreasing in the seaward direction. While the maximum concentrations of Chl-a appear to be fairly consistent seasonally, the spatial extent of blooms has significant seasonal fluctuations. Monthly mean imagery shows the largest spatial coverage of Chl-a in winter and the smallest coverage of the SAB in summer. Chl-a concentration on the inner shelf, with the exception of the southern SAB near Cape Canaveral, is relatively high year-round. We note that some portions of phytoplankton blooms may only occur in subsurface waters, making it impossible to see from satellite imagery.

The seasonal cycle is more evident in the SST field. Temperatures on the shelf in November through April are below 15 °C increasing to ~24 °C in May and reaching a maximum over 28 °C in June through August until decreasing again in September to October. Water temperature in the shallow inner shelf is colder (warmer) than that in the middle shelf in winter (summer). From November to May, there is a drastic temperature difference

(~8–10 °C) between near-shore waters and the GS, whereas SST during summer months is nearly uniform over the entire SAB. Throughout the year, the GS retains relatively stable SSTs (with annual changes of less than 3–4 °C) though it does meander horizontally with a generally offshore mean position in winter and an onshore mean position in summer (Signorini and McClain, 2006).

To highlight regional differences, monthly temperature time-series were constructed by averaging SST values along two shelf transects, one in the northern SAB and the other in the southern SAB (see Fig. 1 for their locations). Time-series results show a clear seasonal cycle in the SST fields for both the northern and southern SAB (Fig. 7). Both regions have similar temperature peaks in summer of ~28 °C, while the northern SAB has deeper temperature troughs in winter, sometimes below 15 °C, which are around 2–3 °C colder than the ~20 °C troughs in the southern SAB. Unlike temperature, Chl-a time-series show a distinctly different regional signal. There is a less clear seasonal cycle in either location. The northern and southern SAB lack any clear relationship and there are higher magnitudes of variability on the southern SAB.

Monthly-mean NARR winds (Fig. 8) show that surface wind in the SAB has a clear seasonal signal, and is generally in agreement with the wind climatology from Blanton et al. (1985). Alongshore northward (upwelling favorable) winds prevail in spring (March–May), and further strengthen in summer (June–August). In fall (September–November), winds change to southwestward, and by Winter (December–February), winds are predominantly eastward and offshore.

USGS river data show that the cumulative river runoff onto the SAB generally peaks in early to mid spring when precipitation is heaviest (there are the occasional exceptions, such as in September of 2004 and September of 2008). River runoff is responsible for the transport of new nutrients to the inner shelf of the SAB and plays an important role in phytoplankton growth and variability (Yoder, 1985, and see Section 5).

### 4. Analysis

To understand intrinsic structures in SAB surface temperature and color fields over six years, we employed the empirical orthogonal function (EOF) analysis on monthly mean SST and Chl-a fields computed from their daily DINEOF reconstructions.

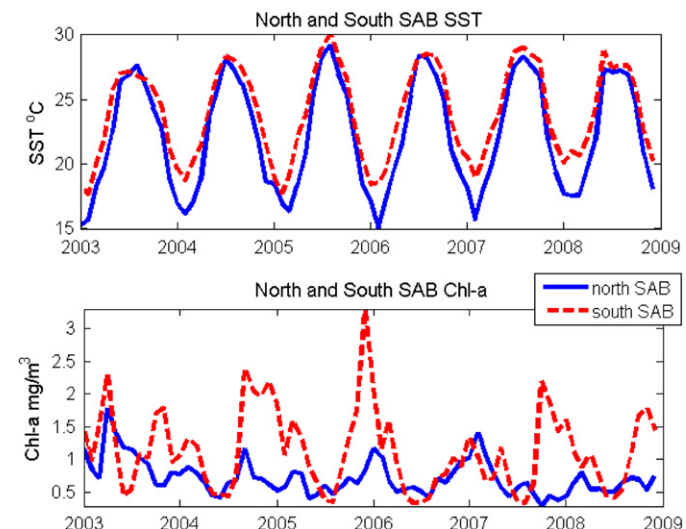


**Fig. 7.** SST (upper panel) and Chl-a (lower panel) monthly means averaged along the north and south SAB transects (locations indicated in Fig. 1).

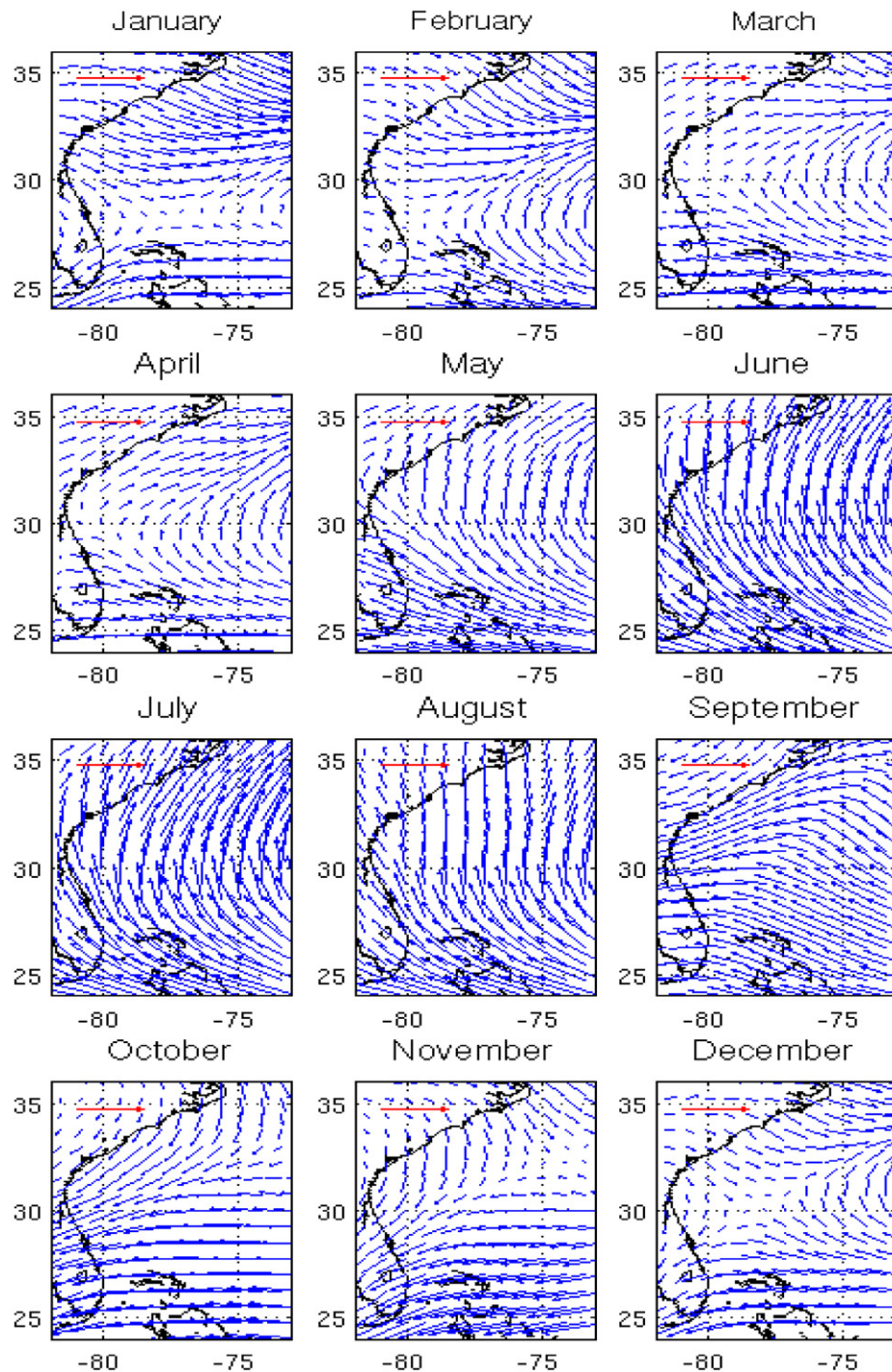


**Fig. 8.** NARR monthly mean wind fields for the SAB, where red vectors denote a wind scale of  $5 \text{ ms}^{-1}$ . (For interpretation of the references to color in this figure legend, the reader is referred to the web version of this article.)

To ensure results are specific to the SAB continental shelf and slope, such EOF analysis was applied on a coastal domain limited to less than the 600 m isobath and from Cape Canaveral to Cape Hatteras, providing temporal (principal components) and spatial (EOF) functions for SST and Chl-*a* fields, respectively.

SST EOF mode 1 (95.75%) is representative of the seasonal solar heating cycle (Fig. 9). The principal component (PC) 1 has a sinusoidal curve that shows warmer temperatures in summer and cooler in winter. Previous studies (e.g., Oey, 1986; He and Weisberg ,2003, among others) show that over seasonal time scales, a one-dimensional balance may express ocean temperature

variation over many shallow shelves:  $\partial T / \partial t = Q / (\rho C_p H)$  where  $Q$  is the net surface heat flux,  $\rho$  the water density,  $C_p$  the water specific heat and  $H$  the local water depth. That is, SST variability is inversely proportional to the water depth. The inner shelf therefore has the largest variability with the highest (lowest) water temperature in summer (winter). Throughout the year, strong heat advection associated with the GS maintains stable temperatures seaward of the shelf break, as demonstrated by the smallest EOF values there.

SST EOF mode 2 (1.74%) (Fig. 9) also has a seasonal cycle, which is likely associated with the combined effects of water stratifica-

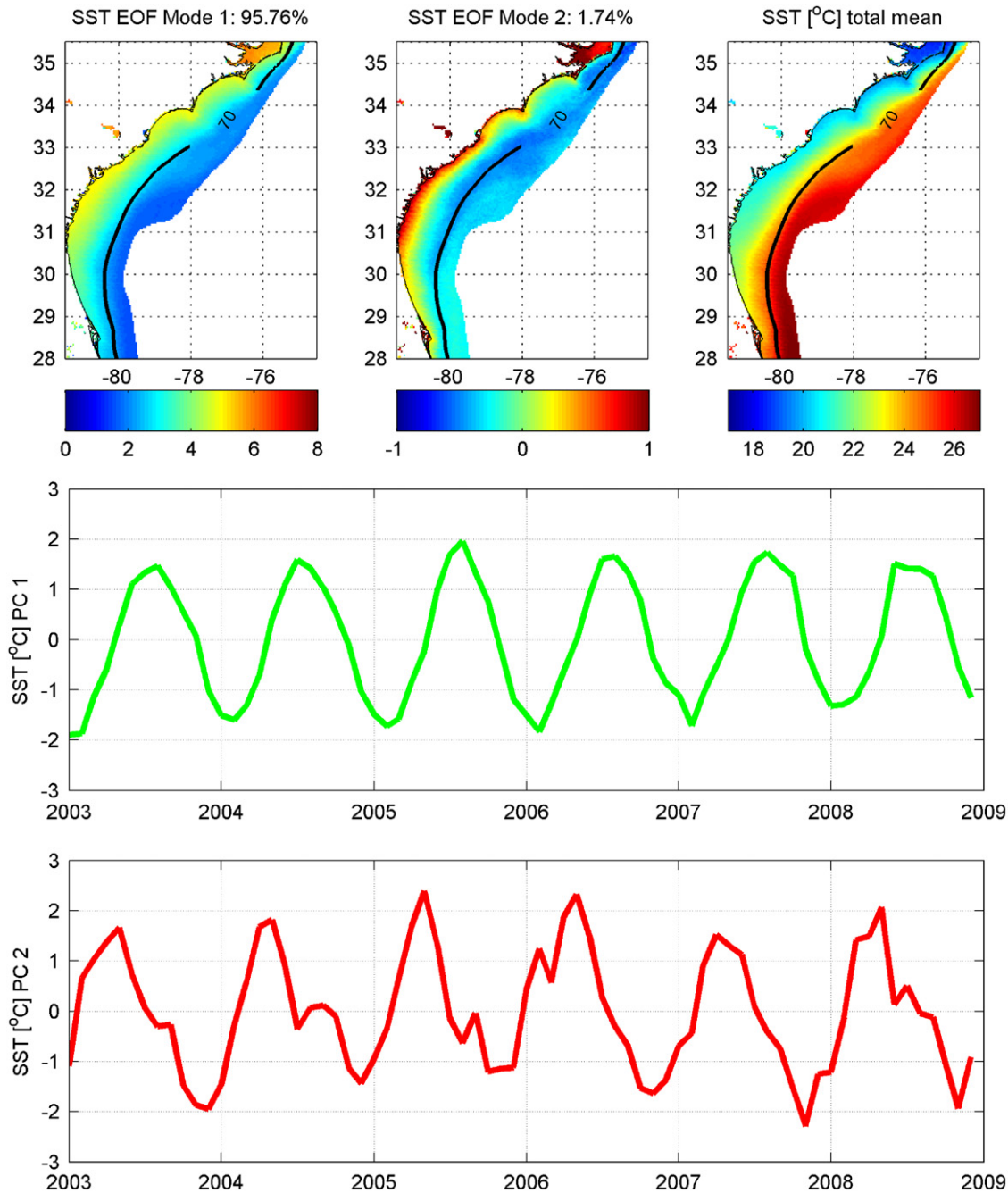


**Fig. 9.** SST EOF mode 1 and 2 (upper left and center panels), the six-year mean (upper right panel) and associated principal components (center and bottom panels). The black contour indicates the 70 m isobath.

tion and surface wind variability as seen in Miles et al., 2009. The PC 2 shows warmest temperatures on the shelf during the highly stratified spring/summer season and coldest temperatures during the well-mixed fall/winter season.

The first Chl-*a* EOF mode (46.35%) has maximum values on the shelf at 32°N, which are out of phase with the southern and northern SAB (Fig. 10). Despite such a regional difference, there is a distinct seasonal signal in Chl-*a* PC 1, similar to SST PC 1. In winter, Chl-*a* concentrations are greater in the southern SAB, off Florida, and in a narrow band on the outer shelf along the entire SAB. In summer months, Chl-*a* concentrations are higher on the shelf off northern Georgia and South Carolina. Indeed, such a result is consistent with observations from raw Chl-*a* time-series (Fig. 7), which show Chl-*a* varies regionally, with concentrations

intermittently out-of-phase. North of 30°N, the shelf widens significantly, and phytoplankton blooms and their associated chl-*a* signatures are largely controlled by local shelf forcing, which contrasts with the southern SAB, near Cape Canaveral and the northern region near the Carolina capes, where the shelf narrows, and the GS plays a more important role in determining circulation and phytoplankton dynamics (Blanton et al., 1981; Yoder, 1985; Yoder et al., 1985).

Unlike the first mode, Chl-*a* EOF mode 2 (10.84%) (Fig. 10) shows a common spatial distribution for the entire SAB shelf. The maximum values occur in the central to northern SAB. Chl-*a* PC 2 lacks any apparent seasonal signal or regular pattern. There is a major bloom event in the spring/summer of 2003, with intermittent peaks throughout the study period. We note the region

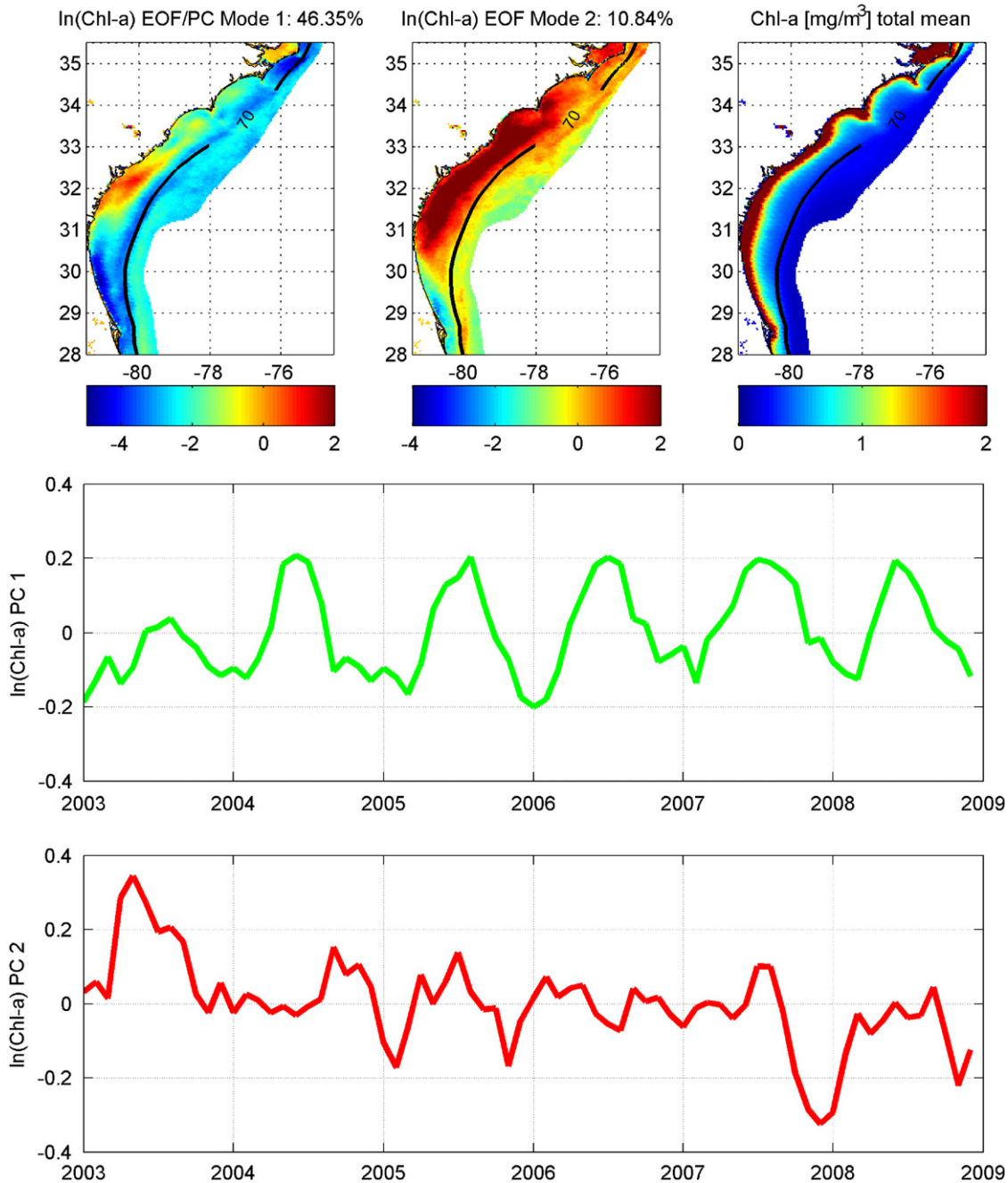


**Fig. 10.** Chl- $a$  EOF modes 1 and 2 (upper left and center panels), its six-year mean in ( $\text{mg}/\text{m}^3$ ) and associated principal components (center and bottom panels). Values are on a natural-log scale; thus negative values correspond to concentrations between 0 and  $1 \text{ mg}/\text{m}^3$  and positive values correspond to concentrations  $> 1 \text{ mg}/\text{m}^3$ . The black contour indicates the 70 m isobath.

represented by positive values in Chl- $a$  EOF mode 2 corresponds to the central SAB, where previous studies have shown river supplied nutrients to be greatest (Atkinson and Menzel, 1985). Indeed, further examinations show Chl- $a$  PC 2 is highly correlated to the cumulative river transport by a one-month lag (Fig. 11). The correlation coefficient between the two time series is 0.65 at a 95% confidence interval. The one-month lag between cumulative river transport and Chl- $a$  PC 2 likely corresponds to the time necessary for heterotrophs to mineralize new riverine nutrients into useable forms for phytoplankton and subsequently for the bloom to develop (Yoder, 1985). While the correlation coefficient is high, we also note peak magnitudes of Chl- $a$  PC2 do not always reflect cumulative river transport peak magnitudes, as other SAB coastal circulation processes may remove nutrients from the

system before phytoplankton can use them for growth. This may be also due to the fact that Chl- $a$  blooms are retained subsurface at times and not evident in satellite imagery.

NARR wind EOF/PC mode 1 (40% of variability) (Fig. 12) shows a clear seasonal cycle. Upwelling favorable (northward) winds dominate the SAB in the spring and summer season, whereas downwelling favorable (southward) winds dominate the SAB in the fall and winter season. Blanton et al. (1985) has shown that large-scale atmospheric systems such as the Bermuda-Azores High drive such seasonal variability. Variations in the north-south wind field play an important role in modifying shelf water properties, as the resulting wind-driven Ekman transport changes signs, modulating cross-shelf transport and nutrient delivery (Atkinson, 1977).

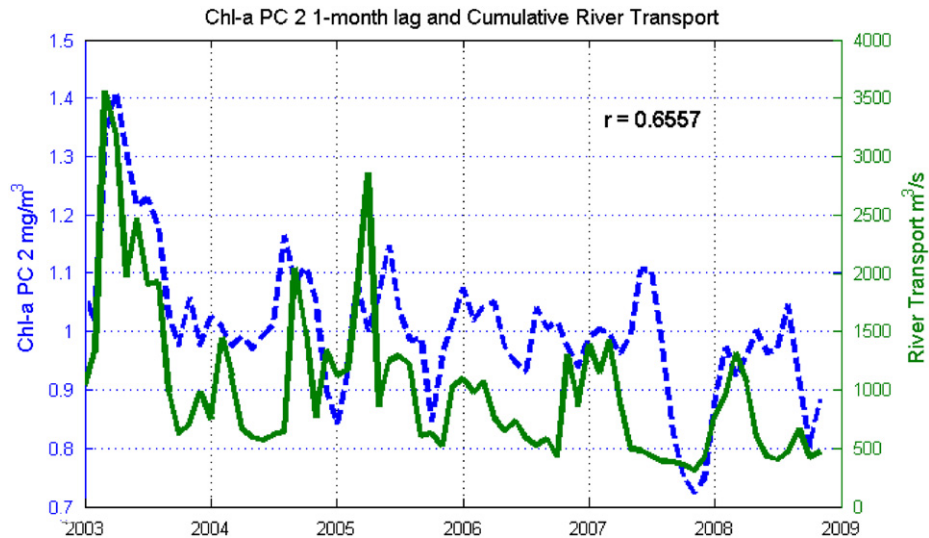


**Fig. 11.** Chl-a PC 2 with a one-month lag (blue dashed line) and the cumulative river transport (green solid line) from the Cape Fear, PeeDee, Altamaha and Savannah rivers. (For interpretation of the references to color in this figure legend, the reader is referred to the web version of this article.)

Wind EOF mode 2 (34% of variability) generally represents east–west winds, which relative to north–south winds, play a smaller role in SAB shelf properties (Lee et al., 1985). Fall and winter winds are relatively strong and predominantly eastward, while spring and summer winds are light and westward.

The linkage between surface wind and SST has been demonstrated in earlier studies. Winds are effective in breaking down the SAB seasonal thermocline and enhancing subsurface GS intrusions. In summer, northward winds can drive surface waters offshore allowing for GS subsurface intrusions to penetrate further onshore in the bottom Ekman Layer (Atkinson, 1977). This process can lead to unseasonably cold temperatures on the outer and middle shelves in summer, such as the cold-water event in summer 2003 (e.g., Aretxabaleta et al., 2006; Miles et al., 2009). It is more difficult to link monthly surface Chl-a concentration with its concurrent wind field directly. Indirect connections through surface wind, cross-shelf nutrient delivery, and shelf-wide Chl-a concentration are however expected.

## 5. Discussion

Barnard et al. (1997) focused on the northern SAB, and showed that Chl-a anomalies led SST anomalies by one month. We saw a similar result when we compared Chl-a PC 1 and one-month lagged SST PC 1 (see Figs. 9 and 10) and found a very robust correlation ( $r=0.84$  at 95% confidence interval). This one-month lag in-phase relationship only holds true for a portion of the central SAB near 32°N. In the remainder of the SAB and offshore waters, there appears to be an out-of phase relationship between SST and Chl-a, which fits with the argument that a stratified water-column in summer would lead to depleted surface chlorophyll and a less stratified water-column in winter would lead to enhanced surface chlorophyll.

Based on our results and previous studies a general explanation of surface Chl-a and SST variability is possible. Studies by Atkinson (1977, 1984) and Yoder et al. (1983, 1985) have shown that the SAB shelf is nutrient depleted, and relies on nutrient pulses from river transport and the GS. These studies also show that SAB nutrient supply from rivers is small compared to short, but powerful nutrient pulses from the GS through eddies, meanders and subsurface intrusions. This finding is supported by our correlation of Chl-a EOF/PC mode 2 with cumulative river

transport (Fig. 11). While being highly correlated between each other, the cumulative river transport explains only ~10% of chlorophyll variability on the SAB.

Lee et al. (1991) show that upwelling in the SAB generally occurs at the shelf-break and that this is a significant source of nutrients to the shelf. We clearly see a narrow band of high variability in the vicinity of the shelf-break in Chl-a EOF mode 1 (Fig. 10). Combined effects of the GS subsurface intrusion and northward winds may explain summer peaks in surface chlorophyll concentrations. GS intrusions occur more frequently in the summer (Atkinson, 1985, Yoder et al., 1985) and work in concert with summer upwelling favorable (northward) wind, which further enhances onshore bottom Ekman transport, allowing GS intrusions to penetrate shoreward to the middle and even inner shelves (Blanton et al., 1981; Signorini and McClain, 2007). Indeed, GS waters have been found at the 30 m isobath off North Carolina, South Carolina, Georgia and northern Florida in the past (Atkinson, 1977). While we cannot see subsurface intrusions from satellite imagery in this study, increased Chl-a concentrations in the summer off Georgia and South Carolina could be related to nutrients and phytoplankton from subsurface intrusions being mixed into surface layers on the inner and middle shelf (Yoder et al., 1985) by strong tidal mixing (Pietrafesa et al., 1985), and topographic upwelling (Janowitz and Pietrafesa, 1982; Atkinson et al., 1977, 1984). More subsurface chlorophyll and nutrient observations are necessary in order to further elucidate the relationships between GS intrusions, wind-driven upwelling and the seasonal variability of chlorophyll on the SAB.

## 6. Conclusion

We reconstructed daily, cloud-free SST and Chl-a imagery for the SAB for a six-year period (2003–2008) using the DINEOF method described in Miles et al. (2009). This is the first long-term DINEOF reconstruction that uses concurrent Chl-a and SST imagery for the SAB. Such reconstructions were used to further calculate monthly means to reflect the regional SST and Chl-a climatology, and to explore seasonal variability of the entire SAB surface ocean. Our analyses not only confirmed the presence of seasonal cycles in both SST and Chl-a, but also highlighted the regional differences between the northern SAB and southern SAB.

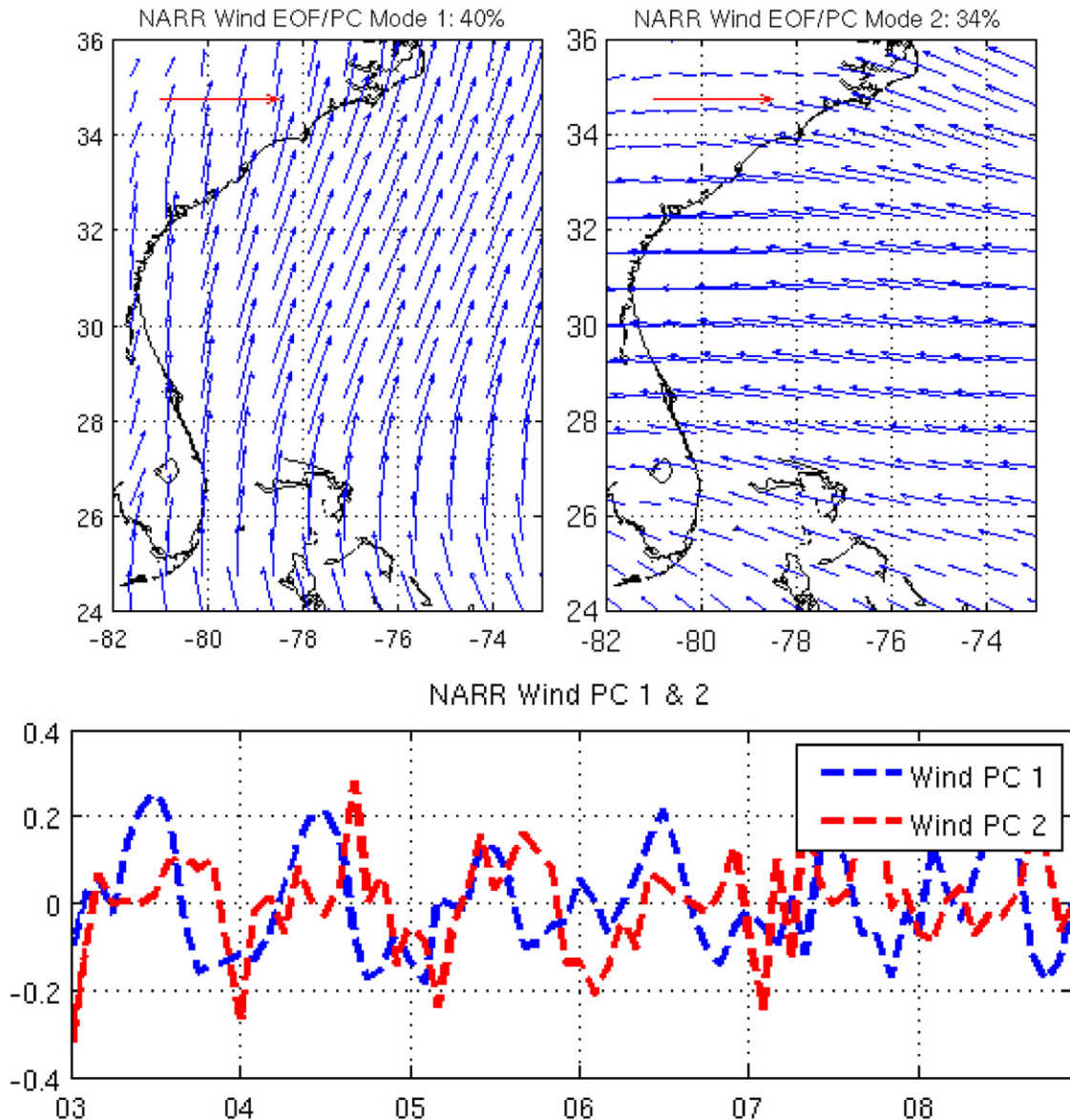


**Fig. 12.** NARR wind EOF modes 1 and 2 and their associated (upper left and right panels) principal components (lower panel). Red vectors denote a scale of  $2.5 \text{ ms}^{-1}$ . (For interpretation of the references to color in this figure legend, the reader is referred to the web version of this article.)

SSTs on the inner shelf have the largest seasonal variability; their values become more stable approaching deeper water and the warm GS. Cross-shelf temperature gradients are strongest in winter and weakest during the summer. In the along-shelf direction, SST variability is more uniform. Water temperature is slightly warmer in the southern SAB than in the northern SAB due to changes in latitudinal solar heating and close proximity of the GS in the southern SAB. We confirmed a robust correlation between mode 1 of Chl-*a* and SST, with SST lagging Chl-*a* by one month on the central to northern SAB. Barnard et al. (1997) first identified this relationship on the SAB, but neither that study nor this study can offer a clear explanation for SST lagging behind Chl-*a*. Further study on subsurface data is necessary to elucidate this phenomenon.

Surface winds in the SAB are largely a function of the location of the Bermuda-Azores High, having an alongshore northward component in summer and southward component in winter. Spring and fall are transitional periods with highly variable cross-shelf winds. Northward (upwelling favorable) winds facilitate GS subsurface intrusions to penetrate further onto the shelf in the

bottom Ekman layer, and on occasion to the inner shelf. We do not see surface expression of these strong upwelling events in monthly mean imagery, though daily SST images (available on our website mentioned in Section 2) in July and August of 2003 particularly, contain evidence of locally reduced temperatures likely due to synoptic GS subsurface intrusion events. Through these intrusions, winds may indirectly enhance nutrient, and thus Chl-*a* concentration on the SAB shelf. In winter, southward downwelling favorable winds keep the SAB well mixed and restrict the development of a strong thermocline until late spring and early summer.

Surface Chl-*a* has highest values on the inner shelf decreasing toward the nutrient depleted GS for all months. Due to shelf-break upwelling, a narrow chlorophyll bloom in the vicinity of the shelfbreak on the outer shelf is often seen. Though monthly mean imagery values show a high concentration of Chl-*a* along the SAB coast, detailed examinations on time-series and regional EOF analysis both show that chlorophyll blooms are highly regionalized between the central and southern SAB. GS and wind variability predominantly force the southern SAB Chl-*a*, while rivers drive the inner shelf Chl-*a* variability on the central SAB

from north Florida to South Carolina. We saw a clear relationship between total river transport and the one-month lagged second mode of Chl-*a* variability, which accounts for ~10% of Chl-*a* variability on the SAB. It is difficult to clearly identify the effects of upwelling on Chl-*a* concentration as satellite imagery is limited to the surface [one optical depth to be more precise; in the coastal ocean in the presence of many forms of organic matter, phytoplankton, sediment and other materials the optical depth is only a few meter deep, see Kirk (1994)] and Chl-*a* blooms may be retained subsurface at the seasonal thermocline. Moreover, chl-*a* field from MODIS sensors are representative of one optical depth. More subsurface nutrient and Chl-*a* observations and three-dimensional coupled biophysical model simulations are necessary to further understand Chl-*a* seasonal variability in the SAB water column.

Overall, the DINEOF method has proved a valuable means for investigating the temporal and spatial variability of SAB surface ocean. The method is robust for studies on continental shelves where intermittent satellite data limits scientists understanding of the oceanographic processes. Application of the DINEOF method to SST and Chl-*a* in the Gulf of Mexico, Mid-Atlantic Bight and other coastal regions with moderate cloud-cover are underway.

## Acknowledgement

We are grateful for the research support NASA provided through Grant NNX07AF62G. We also acknowledge NASA GSFC for providing MODIS data, NCEP NARR for providing wind data, and USGS for providing river flow used in this research.

## Appendix A

We present a concise description of the DINEOF procedure, which is largely from Miles et al. (2009). Interested readers can also refer to Alvera-Azcarate et al. (2007) for a more detailed explanation. First, the initial data input ( $X$ ) is obtained by subtracting the temporal mean and setting the missing data to 0. Second, a singular value decomposition (SVD) of  $X$  is performed. This fills in missing data with a best guess by the equation:  $X_{i,j} = \sum_{p=1}^k \rho_p(u_p)_i(v_p^T)_j$ , where  $i$  and  $j$  in  $X$  are the temporal and spatial indices, respectively,  $k$  is the number of EOF modes,  $\mathbf{u}_p$  and  $\mathbf{v}_p$  are the  $p$ th column of the spatial and temporal functions of EOF, and  $\rho_p$  (where  $p=1,\dots,k$ ) represents the corresponding singular values. Step 2 is repeated iteratively  $k$  times or until convergence, using the previous best guess as the initial value for the subsequent iteration, where convergence is defined by a preset threshold of the absolute value of the difference between the SVD of the current and previous iterations. Third, a cross-validation technique determines the optimum number of EOF modes retained in the reconstruction. Finally, the first and second steps are repeated using only the optimum number of EOF modes and the temporal mean is added to the reconstructed matrix to obtain the interpolated dataset.

Following Alvera-Azcarate et al. (2007), we used a multivariate adaptation of DINEOF in this study. An extended matrix  $X_e$ , which contains multiple state variables, determines the reconstruction. Specifically, we utilized concurrent SST, Chl-*a*, and 1-day-lagged SST to reconstruct SST fields. Similarly, we used Chl-*a*, SST, and 1-day-lagged Chl-*a* to reconstruct Chl-*a* fields. To yield the best reconstruction results, we performed sensitivity experiments to determined lag-time. We found 1-day lag to be ideal for our purposes. In the event that the following day had less than 5% data coverage, we utilized the next closest valid day as the 1-day-lagged data. The DINEOF procedure calculates correlation

between variables internally and no *a priori* knowledge of these relationships is necessary to perform the multivariate reconstruction. After reconstruction, only missing (cloud-covered) data is filled in and original valid data are retained.

## References

- Alvera-Azcarate, A.A., Barth, J.-M., Beckers, Weisberg, R.H., 2007. Multivariate reconstruction of missing data in sea surface temperature, chlorophyll, and wind satellite fields. *J. Geophys. Res.* 112, C03008. doi:10.1029/2006JC003660.
- Aretxabaleta, A., Nelson, J.R., Blanton, J.O., Seim, H.E., Werner, F.E., Bane, J.M., Weisberg, R., 2006. Cold event in the South Atlantic Bight during summer of 2003: anomalous hydrographic and atmospheric conditions. *J. Geophys. Res.* 111, C06007. doi:10.1029/2005JC003105.
- Atkinson, L.P., 1977. Modes of Gulf Stream intrusion into South Atlantic Bight shelf waters. *Geophys. Res. Lett.* 4, 583–586.
- Atkinson, L.P., O'Malley, P.J., Yoder, J.A., Paffenhofer, G.A., 1984. The effect of summertime shelf break upwelling on nutrient flux in southeastern United States continental shelf waters. *J. Mar. Res.* 42, 929–993.
- Atkinson, L.P., 1985. Hydrography and nutrients of the Southeastern U.S. continental shelf. In: Atkinson, L.P. (Ed.), *Oceanography of the Southeastern U.S. Continental Shelf, Coastal and Estuarine Sciences*, 2. AGU, Washington, DC, pp. 77–92.
- Atkinson, L.P., Menzel, D.W., 1985. Introduction: oceanography of the Southeast United States Continental Shelf. In: Atkinson, L.P. (Ed.), *Oceanography of the Southeastern U.S. Continental Shelf, Coastal and Estuarine Sciences*, 2. AGU, Washington, DC, pp. 1–9.
- Barnard, A.H., Stegmann, P.M., Yoder, J.A., 1997. Seasonal surface ocean variability in the South Atlantic Bight derived from CZCS and AVHRR imagery. *Cont. Shelf Res.* 17 (10), 1181–1206.
- Bishop, S.S., Yoder, J.A., Paffenhofer, G.-A., 1980. Phytoplankton and nutrient variability along a cross-shelf transect off Savannah, Georgia, U.S.A. *Estuarine Coastal Mar. Sci.* 11, 359–368. doi:10.1016/S0302-3524(80)80061-2.
- Blanton, J.O., 1981. Ocean currents along a nearshore frontal zone on the continental shelf of the southeastern United States. *J. Phys. Oceanogr.* 11, 1627–1637.
- Blanton, J.O., Atkinson, L.P., Pietrafesa, L.J., Lee, T.N., 1981. The intrusion of Gulf Stream water across the continental shelf due to topographically-induced upwelling. *Deep Sea Res. Part A* 28, 393–405.
- Blanton, J.O., Schwing, F.B., Weber, A.H., Pietrafesa, L.J., Hayes, D.W., 1985. Wind Stress Climatology in the South Atlantic Bight. In: Atkinson, L.P. (Ed.), *Oceanography of the Southeastern U.S. Continental Shelf, Coastal and Estuarine Sciences*, 2. AGU, Washington, DC, pp. 10–22.
- He, R., Weisberg, R.H., Zhang, H., Muller-Karger, F.E., Helber, R.W., 2003. A cloud-free satellite derived, sea surface temperature analysis for the west Florida shelf. *Geophys. Res. Lett.* 30 (15), 1811. doi:10.1029/2003GL017673.
- He, R., Weisberg, R.H., 2003. West Florida Shelf circulation and temperature budget for the 1998 fall transition. *Cont. Shelf Res.* 23 (8), 777–800.
- Janowitz, G.S., Pietrafesa, L.J., 1982. The effects of alongshore variation in bottom topography on a boundary current—topographically induced upwelling. *Cont. Shelf Res.* 1, 123–141.
- Kirk, J.T.O., 1994. Light and Photosynthesis in Aquatic Ecosystems second ed. Cambridge University Press 509 pp.
- Lee, T.N., Yoder, J.A., Atkinson, L.P., 1991. Gulf stream frontal eddy influence on productivity of the Southeast U.S. Continental Shelf. *J. Geophys. Res.* 96 (C12), 22,191–22,205.
- Lee, T.N., Kourafalou, V., Wang, J.D., Ho, W.J., Blanton, J.O., Atkinson, L.P., Pietrafesa, L.J., 1985. Shelf circulation from Cape Canaveral to Cape Fear during winter. In: Atkinson, L.P. (Ed.), *Oceanography of the Southeastern U.S. Continental Shelf, Coastal and Estuarine Sciences*, 2. AGU, Washington, DC, pp. 33–62.
- Miles, T.N., He, R., Li, M., 2009. Characterizing the South Atlantic Bight seasonal variability and cold-water event in 2003 using a daily cloud-free SST and chlorophyll analysis. *Geophys. Res. Lett.* 36, L02604. doi:10.1029/2008GL036396.
- Oey, L.W., 1986. The Formation and Maintenance of Density Fronts on the U.S. Southeastern Continental Shelf during Winter. *J. Phys. Oceanogr.* 16, 1121–1135.
- Oey, L.Y., Atkinson, L.P., Blanton, J.O., 1987. Shoreward Intrusion of Upper Gulf Stream Water onto the U.S. Southeastern Continental Shelf. *J. Phys. Oceanogr.* 17, 2318–2333.
- Pietrafesa, L.J., Blanton, J.O., Wang, J.D., Kourafalou, V., Lee, T.N., Bush, K.A., 1985. The tidal regime in the South Atlantic Bight. In: Atkinson, L.P. (Ed.), *Oceanography of the Southeastern U.S. Continental Shelf, Coastal and Estuarine Sciences*, vol. 2. AGU, Washington, DC, pp. 63–76.
- Ryan, J.P., Yoder, J.A., 1996. Long term mean and even related pigment distributions during the unstratified period in South Atlantic Bight outer margin and middle shelf waters. *Cont. Shelf Res.* 16, 1165–1183.
- Signorini, S.R., McClain, C., 2006. Remote versus local forcing on chlorophyll variability in the South Atlantic Bight. *NASA Tech. Mem.*, 2006–214145.
- Signorini, S.R., McClain, C.R., 2007. Large-scale forcing impact on biomass variability in the South Atlantic Bight. *Geophys. Res. Lett.* 34, L21605. doi:10.1029/2007GL031121.
- Yoder, J.A., 1985. Environmental Control of Phytoplankton Production on the Southeastern U.S. Continental Shelf. In: Atkinson, L.P. (Ed.), *Oceanography of the Southeastern U.S. Continental Shelf, Coastal and Estuarine Sciences*, 2. AGU, Washington, DC, pp. 93–103.

Yoder, J.A., Atkinson, L.P., Bishop, S.S., Hofmann, E.E., Lee, T.N., 1983. Effect of upwelling on phytoplankton productivity of the outer southeastern United States continental shelf. *Cont. Shelf Res.* 1, 385–404. doi:10.1016/0278-4343(83)90004-3.

Yoder, J.A., Atkinson, L.P., Bishop, S.S., Blanton, J.O., Lee, T.N., Pietrafesa, L.J., 1985. Phytoplankton dynamics within Gulf Stream intrusions on the southeastern United States continental shelf during summer 1981. *Cont. Shelf Res.* 4, 611–635.